

FT-IR EMISSION/TRANSMISSION TOMOGRAPHY OF COAL FLAMES

P.R. Solomon, J.R. Markham, Y.P. Zhang, and R.M. Carangelo
Advanced Fuel Research, Inc.
87 Church Street
East Hartford, CT 06108

INTRODUCTION

Fourier Transform Infrared (FT-IR) Emission/Transmission (E/T) spectroscopy has recently been shown to be a versatile technique for coal combustion diagnostics by allowing for measurements of particle concentrations and temperatures, and gas compositions, concentrations, and temperatures (1). These measurements are for the ensemble of particles and gases along a line-of-sight in the flame.

To correct the shortcoming of the line-of-sight measurements, tomography techniques have been applied to both the FT-IR emission and transmission spectra to obtain spatially resolved spectra from which local flame properties can be obtained. This method has been applied to a stable, well defined co-annular laminar ethylene diffusion flame (2,3). From the spatially resolved spectra, point values for species temperature and relative concentrations were determined for CO₂, H₂O, alkanes, alkenes, alkynes, and soot. Temperatures (for CO₂ and H₂O), and soot concentrations were found to be in good agreement with measurements performed on the same flame by coherent-anti-stokes Raman spectroscopy (CARS) (4) and laser scattering (5), respectively.

The technique was recently applied to a coal flame produced in a transparent wall reactor (TWR) using a Rosebud subbituminous coal (6). From these spectra, spatially resolved point values have been obtained for particle and CO₂ temperatures, relative particle, soot and CO₂ concentrations, the fraction of ignited particles, and the relative radiance intensity.

To study the effect of these conditions on coal type, two more flames have now been characterized. These are a second Rosebud subbituminous coal flame produced using a slower flow of preheated gas and a flame using Pittsburgh Seam coal produced under the same conditions. This paper compares the results from these three flames.

EXPERIMENTAL

Apparatus

The TWR facility has been described previously (1,6). The coal is injected upwards into the center of a 10 cm diameter upward flowing preheated air stream in the center of a 20 cm diameter x 70 cm tall glass enclosure. A flow of room temperature air along the perimeter of the reactor keeps the enclosure cool. Radial thermocouple measurements show that the preheated air stream provides a stable hot environment for the coal up to a height of about 30 cm. Our coal feeding system uses a carrier gas which exits the feeder through a tube as it is slowly lowered through a bed of coal particles. Mechanical vibration helps to displace and entrain particles into the tube. A steady feed results in a flame that is stable in shape and position except for the ignition point, where rapid verticle fluctuations of ± 5 mm are observed. The gas flows used for the high flow case were 2.9 l/sec in the preheated gas and 4.2×10^{-3} l/sec in the carrier gas. The gas flows used for the low flow case were 1.7 l/sec in the preheated gas and 3.6×10^{-3} l/sec in the carrier gas. The coal feed rate was 0.91 g/min for both cases.

The enclosure has movable KBr windows to allow access to the flame by the FT-IR spectrometer (a modified Nicolet 20SX). As discussed in Ref. 7, emission measurements are made by directing the radiation emitted by the hot sample stream through an interferometer to an "emission" detector. Transmission measurements are made by replacing this detector with a high intensity global source which, after passing through the interferometer, is directed through the sample area to a "transmission" detector. The emission and transmission measurements are made along the same 1 mm wide by 4 mm high optical path defined with apertures. With this optical geometry, twenty-one parallel line-of-sight emission and transmission spectra were collected across the coal stream at 1 mm increments along the radius for each slice. Several slices were obtained for each flame.

The spatially resolved "point" values correspond to an average within 1 mm x 1 mm x 4 mm high volumes. In this work the data were smoothed by co-adding data from eight adjacent wavenumber bands. This results in degraded resolution from the 8 cm^{-1} used, although still sufficient to quantitatively measure the gas species.

Sample

The samples used in this experiment were sieved fractions (200 x 325 mesh) of dry Montana Rosebud subbituminous coal and dry Pittsburgh Seam coal. The characteristics of these coals have been published previously (1,8).

ANALYSIS

The analysis for the line-of-sight FT-IR E/T measurement pertaining to multi-phase reacting streams has been presented previously (1,6,7,9-11). The relative concentration and temperatures for individual components (gas, soot, and particles) are obtained from the transmission and normalized radiance spectra, respectively, as discussed in Refs. 1,6,7,9-11.

The reconstruction of spatially resolved FT-IR spectra from multiple line-of-sight spectra was first introduced elsewhere (2,3,6). We have employed the standard Fourier image reconstruction technique (12) which is capable of handling data from systems of arbitrary shape. Our flame, however, was cylindrically symmetric. The computer program published by Shepp and Logan was used for this work (12) by applying the reconstruction one wavelength at a time to determine spatially resolved spectra.

A straight-forward application of the reconstruction technique to radiance spectra is not possible, because of self-absorption in the sample. In the case of small absorbance encountered in this work (percent transmission $> 80\%$), an emission measurement can be directly corrected by an absorption measurement made along the same path. A self-absorption correction corresponding to that used by Freeman and Katz was employed for the thin sample studied (13). The Fourier reconstruction program can be applied directly to the emission thus corrected, to obtain local radiances. These are then converted to normalized radiance and the analysis proceeds as for the line-of-sight spectra.

RESULTS

Flame Characteristics

The three flames are presented in Fig. 1. All three flames are characterized by a bright ignition zone followed by a region of lower intensity where burnout is occurring. Photographs show the high intensity zone to contain burning volatile clouds which are 3 to 5 times the diameter of the particles. The Pittsburgh Seam coal shows a region of distinct dimness after ignition which may occur after the initial oxygen is consumed by the volatiles.

Measurements were made of the particle velocities by measuring the length of tracks recorded with a video camera using a 1/250 shutter speed. The results are presented in Fig. 2. The particles accelerate as they leave the nozzle due to the heating of the carrier gas, the influence of the faster hot gas surrounding the carrier gas stream, and buoyancy effects. At ignition, the acceleration is increased as the center stream is rapidly heated. The data show the velocities increasing to above the hot gas velocity. The heating of the central stream appears to dominate the particle velocity as the two cases where the hot gas velocity is lowest (Fig. 2b and 2c) produces a higher particle velocity than in Fig. 2a where the hot gas velocity is higher. Based on these velocities, the particle residence times (given in Fig. 1) were computed.

The tomography data for these three flames are presented in Figs. 3 to 5. The seven parameters which were measured are: a) relative particle and soot concentration, b) the multiplier M which is the emissivity times the fraction of particles at the measured temperature, c) the spectral radiance at 4500 cm^{-1} , d) the particle and CO_2 temperatures, and e) the CO_2 concentration. The tomography data for the Rosebud fast flow case are presented in Fig. 3. These data were presented previously (6) but are reproduced here for comparison. Figure 3a presents the height of

the continuum blockage determined from the transmittance spectra as percent blockage of the incident IR beam. The blockage is divided into particles and soot. Soot is observed to appear at ignition as inferred by the change in shape of the continuum as described below. Below the ignition (6 cm above the 4 mm diameter nozzle) there are particles only (no soot) confined to a radius of about 6 mm. This is in agreement with the boundaries as determined by scattering of a He-Ne laser beam. The multiplier, M (the product of emissivity times the fraction of ignited particles in Fig. 3b shows a few particles (up to 10%) have ignited at the edge of the coal stream. Such ignited particles can also be seen in Figs. 1b and 1c.

Just above ignition (10.5 cm above the nozzle), the particles appear to be forced inward into a more dense central stream at the same time that some particles are spread outward. The spreading of the stream is confirmed visually. This spreading is consistent with the location of the ignition zone centered at about 2 mm radius, indicated by the 0.35 M value in Fig. 3b (i.e., approximately one-third of the particles ignite). Considerably less material is ignited at the center and outer region of the ignition zone. The increase in gas volume in this zone acts to compress the stream inward and expand the stream outward. The total particle blockage (number in parentheses in Fig. 3a) determined by integrating the blockage times area indicates that the blockage is increased from 1.0 (by definition) at 6 cm to 1.7 at 10.5 cm to 1.5 at 12 cm. This suggests that the devolatilization which appears complete at this point may swell or fragment the particles to increase the blockage. Swelling is observed in SEM photographs of collected particles. Above 12 cm, the particle blockage is reduced as the material burns out (Fig. 3a).

The multiplier, M (Fig. 3b), indicates that the ignition zone quickly collapses to the center axis (compare 10.5, 12, and 14 cm). From 14 cm through 16 cm M again drops near the center region, but this may be caused by a build-up of ash in the center region, as evidenced by a corresponding drop in the relative amount of soot compared to particles at these positions. At 20 cm, an increase in blockage at radiuses above 4 mm is observed (ash dispersion) with a corresponding decrease in M above 4 mm and an increase in M at the center.

Figure 3c presents the local radiance determined at 4500 cm^{-1} . At 6 cm, high frequency radiance is detected from the previously mentioned few particles that are observed to ignite at the edge of the coal stream. Just above the ignition point (10.5 cm), the high values of radiance along the center result from the high density of particles blockage, even though M may be low. The radiance from 10.5 cm to 12 cm is observed to increase along the center, as was observed for M.

Figure 3d presents the temperature of CO_2 (dashed line) and total continuum, both particles and soot (solid line). Also presented are measurements with a Pt + PtRh thermocouple obtained in the flame at the 12, 16, and 20 cm positions. The particles have a relatively constant temperature between 1800 and 1900 K at 10.5 and 12 cm. The cooler center region at 10.5 cm (in agreement with M and radiance) is observed. Particle temperature increases from 1900 K to 2000 K at 14 cm, and to 2200 K to 2400 K through 16 to 20 cm. Above 20 cm the temperature falls.

The maximum CO_2 temperatures (2200 to 2600 K) occur in the regions of high particle radiance where the maximum combustion is occurring, although the center temperature at 12 and 16 cm are puzzling. In the beginning region of the flame, CO_2 is 400 to 700 K hotter than the particles in the same region suggesting that CO is burning to CO_2 away from the particles. CO_2 temperatures are generally closer to the particle temperatures above 14 cm. At the edge of the stream the CO_2 temperature is always lower due to rapid heat transfer to the surrounding air. At 20 cm the CO_2 and particle temperatures are within 100 K except along the axis where the CO_2 is hotter.

The CO_2 concentrations are presented in Fig. 3e. Below ignition the CO_2 concentration is very small. Above ignition the CO_2 level jumps drastically and spreads with increasing height. These data present a picture of the coal burning in a shrinking region which collapses to the center at the tip of the flame.

The results for the two other flames are presented in Figs. 4 and 5. The trends are qualitatively similar. There are, however, differences in the soot formation, swelling, ignition, particle temperatures, burnout, and CO_2 concentrations, and these will be discussed below.

Soot Formation - As described previously (1) the shape of the continuum spectra can be employed to separate the contributions from particles and soot. Two spectra for the Pittsburgh Seam coal are presented in Fig. 6. Figure 6a presents $1-\tau$, where τ is the transmittance, prior to ignition where no soot is present. The upward slope toward low wavenumbers (long wavelengths) is due to diffraction. Figure 6b presents a spectrum above ignition in the region of high soot. The spectrum now slopes in the opposite direction due to soot. To resolve the spectrum into particle and soot contributions, the frequency dependent extinction efficiency, F_p , for the particles (which is proportional to $(1-\tau)$) is assumed to have the same shape as prior to ignition, and the particle transmittance is assumed to be equal to the measured transmittance extrapolated to 0 cm^{-1} (where the attenuation from soot goes to zero). A straight line extrapolation is made below 3500 cm^{-1} excluding the region of the spectrum containing CO_2 and H_2O bands. The soot contributions is the difference between the particle attenuation and the total as shown in Fig. 6c.

The relative amounts of soot can be seen in Figs. 3a, 4a, and 5a. The soot concentration is highest just above ignition. The highest soot concentrations are observed for the Pittsburgh Seam coal followed by the Rosebud slow case and then the Rosebud fast case. For Pittsburgh Seam, the highest attenuation from soot is about three times that from the particles. For Rosebud (slow flow) the highest value is only 2.3 times and for Rosebud (fast flow) only a little over 1 times. The variation in soot concentration comes from two factors: 1) tar, which is the soot precursor (1) is higher for Pittsburgh Seam coal than for Rosebud, and 2) the better mixing in the fast flow increases the oxygen to the central core which reduces the soot.

Swelling and Fragmentation - The swelling or fragmentation of the particles is indicated by the integrated particle blockage values as a function of position. The 6 cm case of the Rosebud and the 4 cm case for the Pittsburgh Seam provide the baseline before ignition. Both cases show a flat distribution over the center 2 mm and goes to zero between 4 and 5 mm. The integrated blockage is given in parenthesis on each of the figures.

If there was no swelling or fragmentation, the blockage would decrease due to the gas heating. For the Pittsburgh Seam coal, the integrated blockage more than triples. Photomicrographs of samples collected in the flame show both swelling of coal and the appearance of small ash particles. Both changes would increase the blockage. For the Rosebud coal, the increases are more modest. While swelling was observed for the fast flow case, the slow flow case does not indicate an obvious swelling or rounding.

Ignition - Ignition for all three cases occurs with the outside of the particle stream (which is in best contact with the hot gases) igniting first. This can be seen in the multiplier M , which is the fraction of ignited particles, in Figs. 3b, 4b, and 5b. At ignition, M is highest at the edge of the particle stream. A photograph in Fig. 7 looking at the ignition zone of the Rosebud slow case clearly shows the ring of ignition. The Pittsburgh which is also a slow flow case exhibits a similar ring while the faster flow case which appears to have better mixing shows the same effect but to a lesser degree. Ignition at the edges is consistent with the particle temperatures below ignition (Fig. 5d) which indicate that the particles at the edge of the stream have reached 800 K while those in the center are as low as 600 K.

Temperatures - The following observations can be made about particle temperatures. 1) Particle temperatures are highest at the edge of the flame where the concentration of oxygen is highest. 2) The lowest temperatures are observed for the Pittsburgh Seam coal, while the highest temperatures are observed for the fast flow Rosebud case. Particle temperatures are generally in the range 1400 to 2200 K.

CO_2 temperatures are always higher than the particle temperatures in the combustion region suggesting that most CO_2 is produced away from the particle surface (e.g., by CO oxidation). The highest CO_2 temperatures were observed in the fast flow case and approached 2600 K.

Burnout - The percent weight loss as a function of distance above the nozzle for the three flames is indicated in Fig. 1, and plotted in Fig. 8. Both slow flow cases display a transient plateau in their burnout profiles which begin within 5 cm past their respective ignition points. Rapid oxygen consumption and inadequate mixing of the surrounding air is believed to cause this effect, which is not displayed for the fast flow (better mixing) case. Both Rosebud flames exhibit essentially 100%

DAF burnout by 50 cm above the nozzle. The Pittsburgh flame, however, seems to contain - 10% char which displays a very low reactivity.

CO₂ Concentration - The concentration of CO₂ for all cases generally decreased with distance away from the centerline for each slice. The slow flow Rosebud case showed an overall larger amount of CO₂ in the combustion region than the fast flow Rosebud case, but this may be attributed to less mixing (and hence, less dilution) for the slow flow condition.

CONCLUSIONS

Tomographic reconstruction techniques have been applied to FT-IR E/T measurements to derive local values for species temperatures and concentrations within three laboratory scale coal flames. Values for particle temperature, relative particle density, relative soot concentration, the radiance intensity, the relative CO₂ concentration and the CO₂ temperature have been obtained as functions of distance from the flame axis and height above the coal injector nozzle. The spectroscopic data are in good agreement with visual observations and thermocouple measurements. These data present a picture of the coal burning in a shrinking region which collapses to the center at the tip of the flame. CO₂ temperatures are highest in the rapid burning zone (2200 to 2600 K). The highest particle temperatures in this zone are 1900 to 2000 K, with temperatures up to 2400 K outside the zone. The three flames showed both coal and flow dependent phenomena. The slow flow cases showed reduced mixing (more soot and more variations in flame properties with radius) compared to the fast flow case. The Pittsburgh Seam coal showed higher soot, higher swelling, lower particle temperatures, and lower char reactivity compared to the Rosebud coal.

ACKNOWLEDGEMENT

This work was supported under the U.S. Department of Energy, Morgantown Energy Technology Center Contract No. DE-AC21-86MC23075. Richard Johnson is the METC Project Manager.

REFERENCES

1. Solomon, P.R., Chien, P.L., Carangelo, R.M., Best, P.E., and Markham, J.R.: Twenty-Second Symposium (International) on Combustion, p. 211, The Combustion Institute, (1988).
2. Chien, P.L., Best, P.E., Carangelo, R.M., and Solomon, P.R., "Tomographic Reconstruction of Fourier Transformed Infrared (FT-IR) Spectra at Points within a Coannular Flame", poster session 22nd Symposium (Int) on Combustion, Seattle, Washington, DC, (Aug. 1988).
3. Best, P.E., Chien, P.L., Carangelo, R.M., Solomon, P.R., Danchak, M. and Ilovici, I.: "Tomographic Reconstruction of FT-IR Emission and Transmission Spectra in a Sooting Laminar Diffusion Flame: Species Concentrations and Temperatures", Combustion and Flame, submitted for publication (1989).
4. Boedeker, L.R., and Dobbs, G.M., Comb. Sci. Technol., 46:301, (1986).
5. Santoro, R.J., Semerjian, H.G., and Dobbins, R.A., Combustion and Flame, 51:203, (1983).
6. Markham, J.R., Zhang, Y.P., Carangelo, R.M., and Solomon, P.R., "FT-IR Emission/Transmission Tomography of a Coal Flame", 23rd Symposium (Int) on Combustion, France, (July 1990).
7. Best, P.E., Carangelo, R.M., and Solomon, P.R.: Combustion and Flame 66, 47, (1986).
8. Serio, M.A., Hamblen, D.G., Markham, J.R., and Solomon, P.R.: Energy & Fuel, 1, 138, (1987).
9. Solomon, P.R., Carangelo, R.M., Best, P.E., Markham, J.R., and Hamblen, D.G.: Twenty-first Symposium (International) on Combustion, p. 437, The Combustion Institute, (1987).
10. Solomon, P.R., Best, P.E., Carangelo, R.M., Markham, J.R., Chien, P.L., Santoro, R.J., and Semerjian, H.G.: Twenty-first Symposium (International) on Combustion, p. 1763, The Combustion Institute, (1987).
11. Solomon, P.R., Carangelo, R.M., Best, P.E., Markham, J.R., and Hamblen, D.G.: Fuel 66, 897, (1987).
12. Shepp, L.A. and Logan, B.F.: IEEE Trans. Nucl. Science, NS-21, (1974).
13. Freeman, M.P. and Katz, S.J.: Optical Society of Am., 50, (8), 826, (1960).

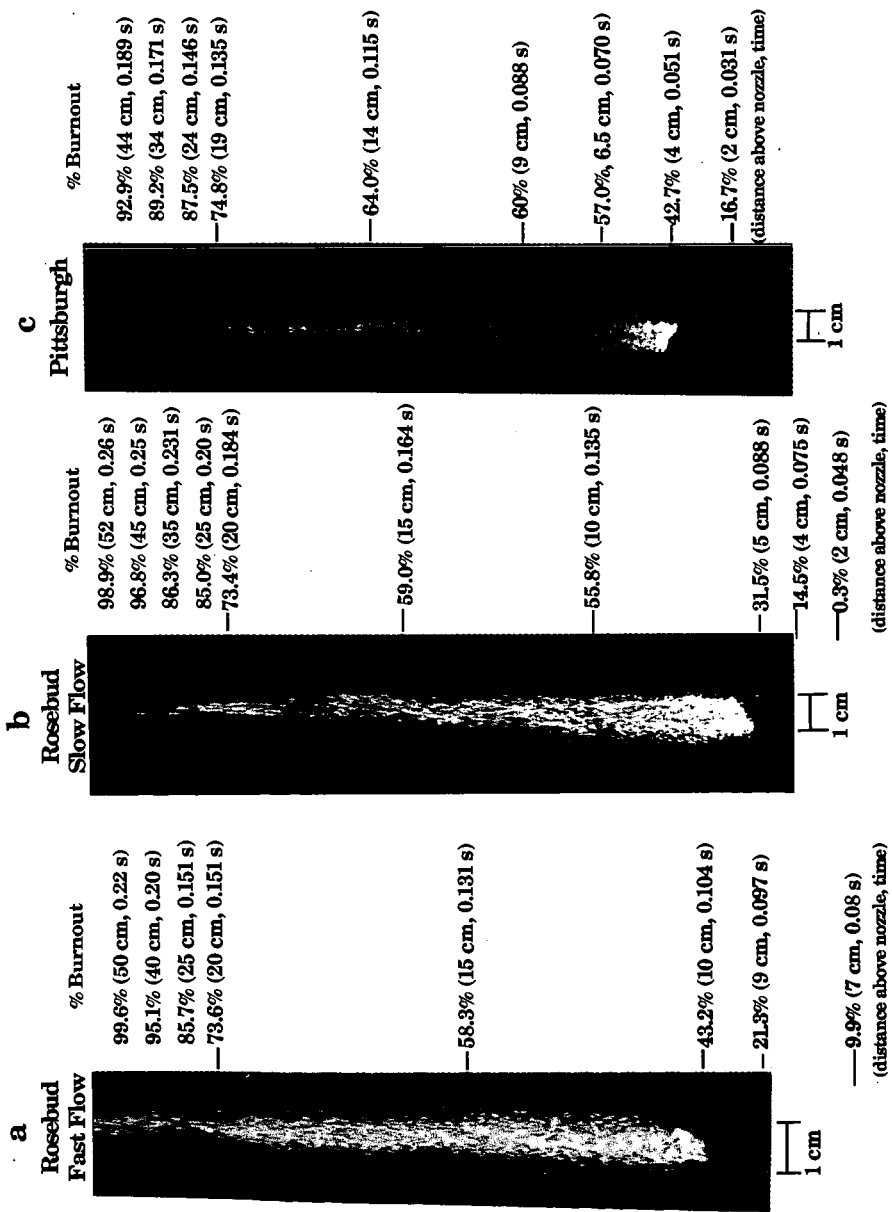


Figure 1. Photographs of Coal Flames in the TWR. a) Rosebud Subbituminous - Fast Flow, b) Rosebud Subbituminous Coal - Slow Flow, and c) Pittsburgh Seam Bituminous - Slow Flow. % Burnout as Determined from Particle Collections in each Flame is Indicated.

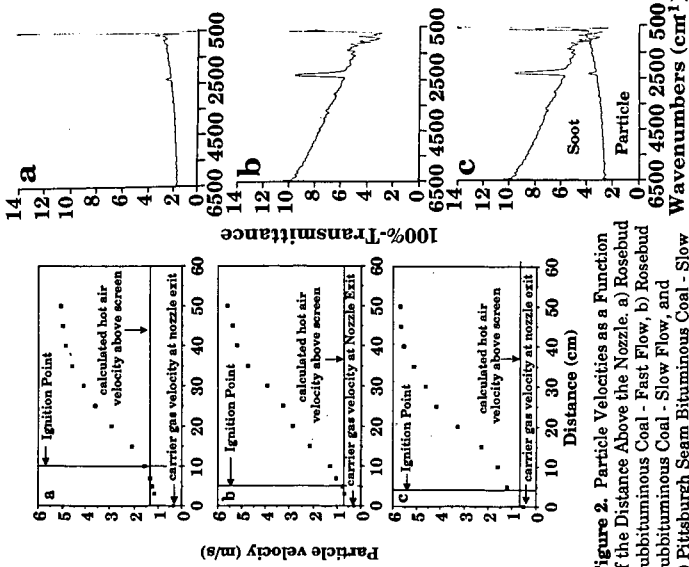


Figure 2. Particle Velocities as a Function of the Distance Above the Nozzle. a) Rosebud Subbituminous Coal - Fast Flow, b) Rosebud Subbituminous Coal - Slow Flow, and c) Pittsburgh Seam Bituminous Coal - Slow Flow.

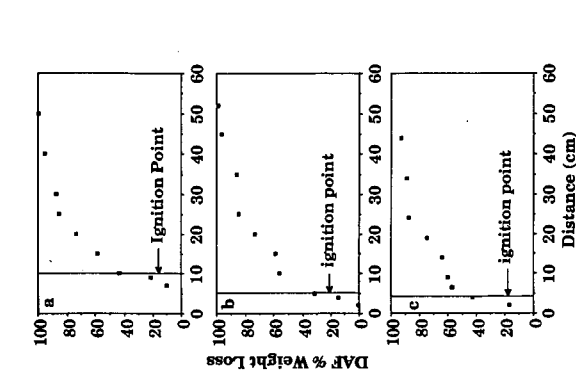


Figure 8. DAF % Weight Loss (burnout) as a Function of Distance Above the Nozzle for a) Rosebud Coal - Fast Flow, b) Rosebud Coal - Slow Flow and c) Pittsburgh Coal - Slow Flow.

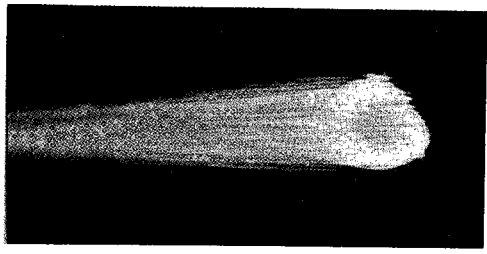


Figure 7. Photograph of Rosebud Subbituminous Coal - Slow Flow Flame Taken from Above the Ignition Region.

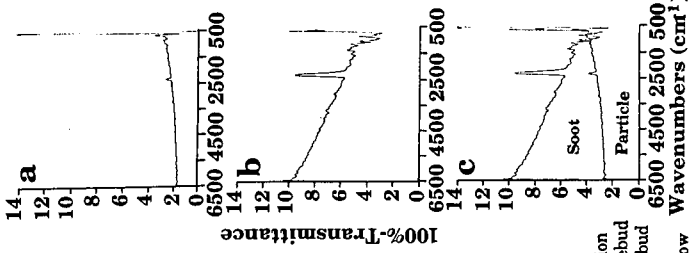


Figure 6. Analysis to Resolve Continuum Blockage Spectrum into Particle and Soot Contributions. a) Particle Blockage Below Ignition, b) Total Particle and Soot Blockage above Ignition, and c) Contribution of Each Component to Total Blockage.

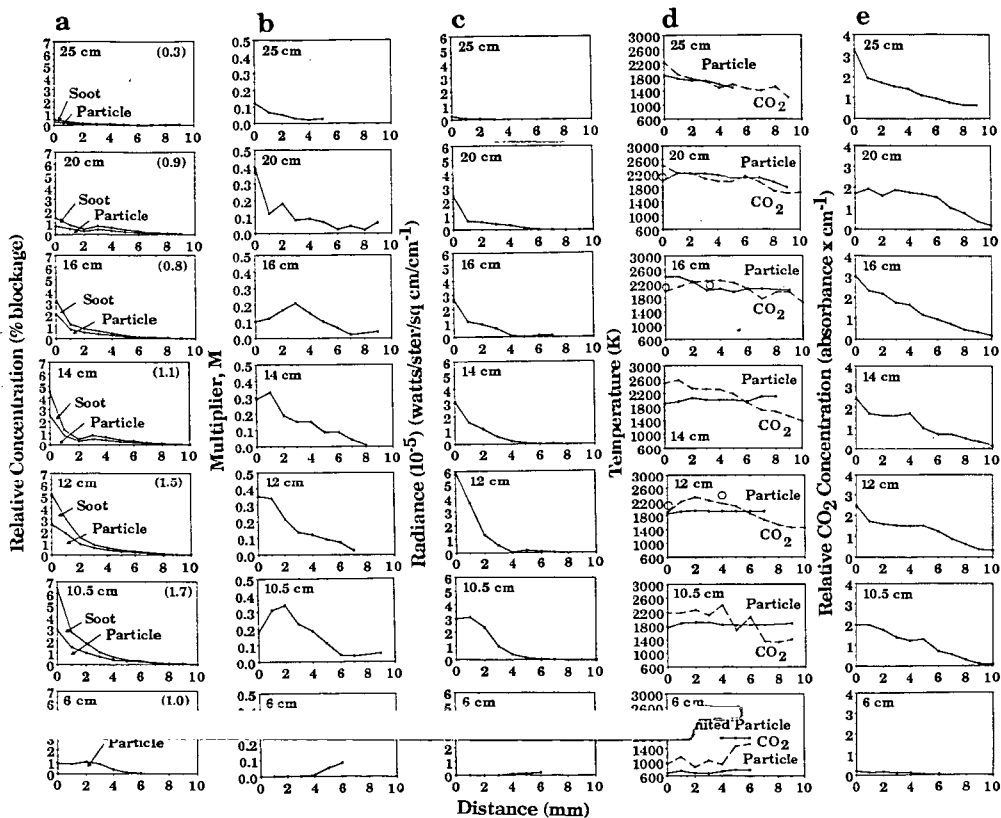


Figure 3. Data for Rosebud Subbituminous Coal - Fast Flow Flame. Radial Distributions of a) Particle and Total (particle + soot) Concentration. Integrated Particle Blockage is Indicated in Parenthesis; b) Multiplier for Ignited Particles (Black-body intensity); c) Spectral Radiance at 4500 cm^{-1} ; d) Particle (solid) and CO₂ (dashed) Temperature; e) CO₂ Concentration at Indicated Distances above the Nozzle for a Rosebud Coal Flame in the TWR.

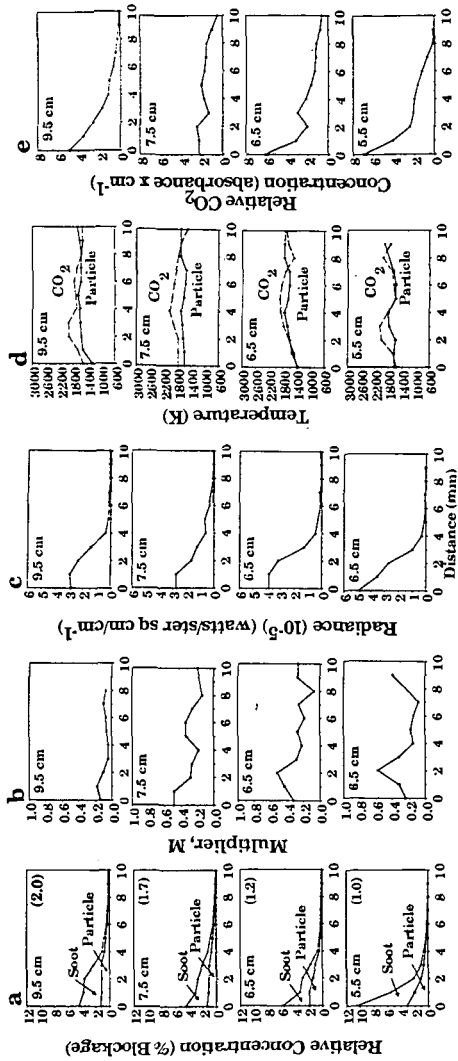


Figure 4. Data for Rosebud Subbituminous Coal - Slow Flow Flame. Radial Distributions of a) Particle and Total (particle + soot) Concentration. Integrated Particle Blockage is Indicated in Parenthesis; b) Multiplier for Ignited Particles (Black-body intensity); c) Spectral Radiance at 4500 cm^{-1} ; d) Particle (solid) and CO_2 (dashed) Temperature; e) CO_2 Concentration at Indicated Distances above the Nozzle for a Rosebud Coal Flame in the TWR.

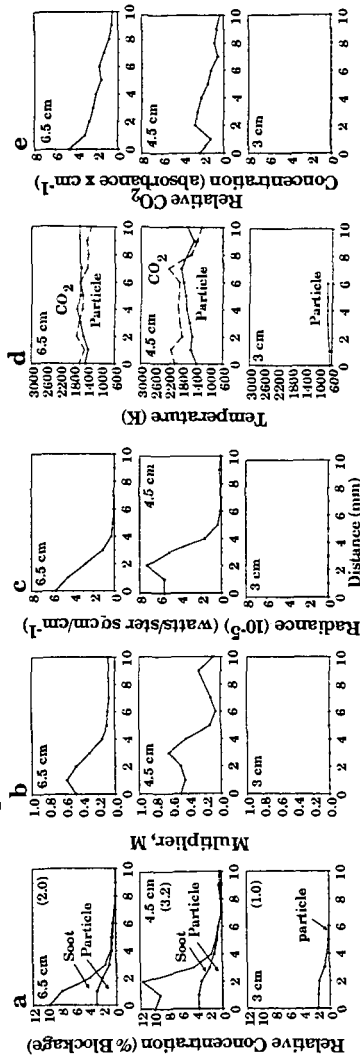


Figure 5. Data for Pittsburgh Seam Bituminous Coal - Slow Flow Flame. Radial Distributions of a) Particle and Total (particle + soot) Concentration. Integrated Particle Blockage is Indicated in Parenthesis; b) Multiplier for Ignited Particles (Black-body intensity); c) Spectral Radiance at 4500 cm^{-1} ; d) Particle (solid) and CO_2 (dashed) Temperature; e) CO_2 Concentration at Indicated Distances above the Nozzle for a Rosebud Coal Flame in the TWR.